Cancer Research

Kallikrein-Related Peptidase 7 Promotes Multicellular Aggregation via the $\alpha_5\beta_1$ Integrin Pathway and Paclitaxel Chemoresistance in Serous Epithelial Ovarian Carcinoma

Ying Dong[1], Olivia L. Tan[1], Daniela Loessner[1], Carson Stephens[1], Carina Walpole[1], Glen M. Boyle[2], Peter G. Parsons[2], and Judith A. Clements[1]

Abstract

Kallikrein-related peptidase 7 (KLK7) is upregulated in epithelial ovarian carcinoma (EOC) with high levels correlated with poor prognosis. However, the mechanisms underlying this relationship and the role of KLK7 in EOC progression are unknown. We report that two different *KLK7* transcripts, *KLK7-253* and *KLK7-181*, are simultaneously expressed in high-grade serous EOC. Multicellular aggregates (MCA), which promote cell survival and chemoresistance, were observed in SKOV-3 cells stably overexpressing KLK7-253 in particular. Importantly, these MCAs invade into a monolayer of mesothelial cells and form cancer cell foci. Blocking MCA using antibodies against KLK7 and $\alpha_5\beta_1$ and β_1 integrins confirmed the involvement of KLK7 and integrin-regulated cell adhesion. Increased levels of α_5/β_1 integrins and enhanced attachment to fibronectin and vitronectin, which was blocked with an anti–β_1 integrin antibody, were also observed. Finally, Western blot and immunohistochemistry showed higher KLK7 and α_5/β_1 integrin levels in serous EOC cells from ascites and tumor samples from chemotherapy nonresponders with short postsurvival times. Additionally, both KLK7-253 and KLK7-181 clones were more resistant to paclitaxel treatment *in vitro*. These findings suggest a mechanism for the association of high KLK7 levels with chemoresistance and poor prognosis for serous EOC patients by promotion of peritoneal dissemination and reinvasion via increased MCA and $\alpha_5\beta_1$ integrin–dependent cell adhesion. *Cancer Res; 70(7); 2624–33. ©2010 AACR.*

Introduction

Ovarian cancer is the leading cause of death from gynecological malignancies, with serous epithelial ovarian carcinoma (EOC) being the predominant subtype. Late diagnosis and chemoresistance result in a ~30% 5-year survival rate (1). Unlike other solid tumors, hematogenous metastasis rarely occurs in ovarian cancer; instead, EOC cells exfoliate from the primary site, form multicellular aggregates (MCA)/spheroids to aid survival in the peritoneal fluid, adhere to mesothelial cells on the surface of the peritoneum, invade into the underlying extracellular matrix (ECM), and grow secondary tumors (2, 3).

Authors' Affiliations: [1]Hormone Dependent Cancer Program, Institute of Health and Biomedical Innovation and School of Life Sciences, Queensland University of Technology, Kelvin Grove, Queensland, Australia and [2]Drug Discovery Group, Division of Cancer and Cell Biology, Queensland Institute of Medical Research, Herston, Queensland, Australia

Note: Supplementary data for this article are available at Cancer Research Online (http://cancerres.aacrjournals.org/).

Y. Dong, O.L. Tan, and D. Loessner contributed equally to this work.

Corresponding Author: Judith A. Clements, Hormone Dependent Cancer Program, Institute of Health and Biomedical Innovation, Queensland University of Technology, 60 Musk Avenue, Kelvin Grove, Queensland 4059, Australia. Phone: 61-7-3138-6198; Fax: 61-7-3138-6039; E-mail: j.clements@qut.edu.au.

doi: 10.1158/0008-5472.CAN-09-3415

Dynamic modulation of cell adhesion molecules, such as integrins, plays a critical role in remodeling the malignant ovarian epithelium during peritoneal metastasis (4). Clinically, high levels of α_v (5) and α_5 (6) integrins are associated with poor outcome. Integrin signaling has been related to MCA/spheroid formation (7) and disaggregation (8) in EOC, and spheroids formed in three-dimensional suspension are more resistant to chemotherapy than two-dimensional monolayer cultured cells (9). Integrins can promote EOC cell dissemination and implantation in the peritoneal cavity via E-cadherin ectodomain shedding (10), loss of E-cadherin (6), and ECM protein degradation (11) by matrix metalloproteinases (MMP). However, the role of other proteases in EOC remains largely unknown.

The kallikrein-related peptidase (KLK) family comprises 15 serine proteases, with several members upregulated in EOC (12–14), including KLK7 (15–20), which is associated with poor prognosis in EOC patients (17, 18). KLKs degrade ECM molecules such as fibronectin and cell adhesion proteins contributing to skin desquamation (21) as well as activate growth factors and other proteases (12–14). Two KLK7 transcripts (KLK7-253 and KLK7-181) have been detected in cancerous but not normal ovarian epithelial (NOE) cells, implying cancer-specific expression (15), although little is known about their biological function in EOC. We now report that stable expression of KLK7-253 and KLK7-181 in SKOV-3 cells promotes paclitaxel resistance and enhances expression of

α_5/β_1 integrins. The KLK7-253 clones, in particular, also form large compact spheroids, which were blocked by functional antibodies against KLK7 and α_5/β_1 integrins and which were capable of invasion into mesothelial cell monolayers. These data provide a mechanism for our clinically observed high KLK7 levels that were associated with chemoresistance and poor outcome.

Materials and Methods

Materials

Antibodies were purchased from Chemicon (integrins), R&D Systems (KLK7), and Invitrogen (anti-V5 and anti-mouse Alexa Fluor 488/568–conjugated secondary antibodies). All other chemicals were purchased from Sigma except where noted below.

Cell lines and ovarian tissue RNA

Cell lines were purchased from the American Type Culture Collection (serous EOC: SKOV-3, OVCAR3, OV-90, and Caov-3; fibroblast: NFF1) or Coriell Cell Repositories (peritoneal mesothelial: LP9) with PEO1, PEO4, PEO14, OAW42, JAM, and CI-80-13S as described previously (15). Other cell lines were generous gifts from Dr. Nelly Auersperg (University of British Columbia, Vancouver, British Columbia, Canada; IOSE144, IOSE379, and IOSE7576) and Dr. Samuel Mok (Harvard University, Cambridge, MA; HOSE17.1, OVCA420, and OVCA432). Four normal ovarian, 31 serous EOC tissue (22), and 7 EOC RNA (15) samples were described previously. Clinical and pathologic information of EOC patients was obtained from the Royal Brisbane Women's Hospital (Supplementary Table S1). Ethical approval was obtained from institutional ethics committees, and informed consent was obtained from all patients.

RNA extraction, reverse transcription-PCR, and reverse transcription-quantitative PCR

RNA was isolated using the RNeasy kit (Qiagen), treated with DNaseI (Invitrogen), and 2 μg RNA reverse transcribed using SuperScript III (Invitrogen). All *KLK7*-specific primers are shown schematically in Fig. 1A, and sequences of all primers, *KLK7* microarray probe, and PCR conditions are listed in Supplementary Table S2. K75'S and K7Ex3AS were used to amplify both *KLK7-253* (573 bp) and *KLK7-181* (442 bp; Fig. 1A). PCR products were sequenced (Australian Genome Research Facility) to confirm transcript-specific amplicons (tBLASTN).

Quantitative PCR (qPCR) was performed on an ABI 7300 thermal cycler (Applied Biosystems) using SYBR Green following the manufacturer's instructions. *KLK7* expression was normalized to *18S* using the standard curve method. K7Ex1qS and K7Ex2qAS primers were used to amplify *KLK7-253*, whereas both *KLK7-253* and *KLK7-181* transcripts (total *KLK7*) were amplified with K7Ex4qS and K7Ex5qAS primers (Fig. 1A). The copy number of *KLK7-181* was obtained by subtraction of *KLK7-253* from total amplified *KLK7*. Microarray analysis was performed as previously described (22).

Generation of stable cell lines

KLK7-253 and KLK7-181 constructs are shown in Supplementary Fig. S1A. *KLK7-253* and *KLK7-181* (Fig. 1A) were amplified from OVCAR3 cDNA, subcloned (pcDNA3.1/V5-His, Invitrogen; COOH-terminal V5 tag), and transfected into SKOV-3 cells using Lipofectamine 2000 (Invitrogen). Monoclonal cells expressing KLK7 or vector control were selected using G418 (Invitrogen). Reverse transcription-qPCR (RT-qPCR) was performed using K7Ex4qS and K7Ex5qAS primers, and products were sequenced confirming transcript-specific expression.

Immunofluorescent microscopy

Cells were grown on coverslips to ~80% confluence, fixed [4% (w/v) paraformaldehyde], blocked [1% (w/v) bovine serum albumin/PBS], and incubated with anti-V5 antibody (1:500). Alexa Fluor 568 phalloidin (Invitrogen) was included with the secondary antibody (Alexa Fluor 488 anti-mouse IgG). Images were taken using a Leica-TCS SP5 confocal microscope (63× 1.4 oil immersion objective) and associated software.

In vitro functional assays

Proliferation assay. Cells (2×10^3 per well) were seeded in phenol red–free RPMI 1640/10% (v/v) FCS in 96-well plates (Nunc) and incubated at 37°C for 4, 24, 48, 72, and 96 h. WST-1 assays were performed per the manufacturer's instructions (Roche). The 4-h time point was used as "no-proliferation" control. The assay was performed thrice with eight replicates per clone per time point.

Cell survival after cisplatin/paclitaxel treatment. Twenty-four hours after seeding, cells were treated with cisplatin (0, 1, 5, 10, 50, and 100 μmol/L) or paclitaxel (0, 0.01, 1, 10, and 100 nmol/L). WST-1 assays were performed 72 h after treatment as above. Cell survival was calculated as percentage of absorbance in nontreated cells.

MCA/spheroid formation and inhibition. Generation of spheroids and MCA inhibition was based on the liquid overlay technique (7). Cells (5×10^3 per well) were layered on top of agarose-coated plates [60 μL of 0.5% (w/v) agarose/serum-free medium] and incubated at 37°C. For MCA inhibition, cells were resuspended in serum-free culture medium, and 5×10^3 cells per well were plated in agarose-coated 96-well plates. Blocking antibodies (anti-$\alpha_5\beta_1/\beta_1$ integrins and anti-KLK7) or control mouse IgG was added (10 μg/mL). Cells were cultured for 2 d and images were taken using a Nikon Eclipse TE2000-U digital camera (4× objective) and V++ software. The experiment was repeated thrice in quadruplicate.

Cell survival of MCA/spheroids after paclitaxel treatment. Spheroid formation was conducted as described above. After 4 d of suspension, cultures were treated with paclitaxel (0, 0.01, 1, 10, and 100 nmol/L), and after 72 h, alamarBlue (Invitrogen) was added [10% (v/v) final concentration] for 5 h per the manufacturer's instruction. Fluorescence was detected using a BMG PolarStar plate reader. The assay was performed thrice with triplicates per clone per concentration. Cell survival was calculated as percentage of fluorescence in nontreated cells.

Monolayer mesothelial cell invasion. LP9 mesothelial cells (5×10^3) were seeded in 96-well plates and grown to

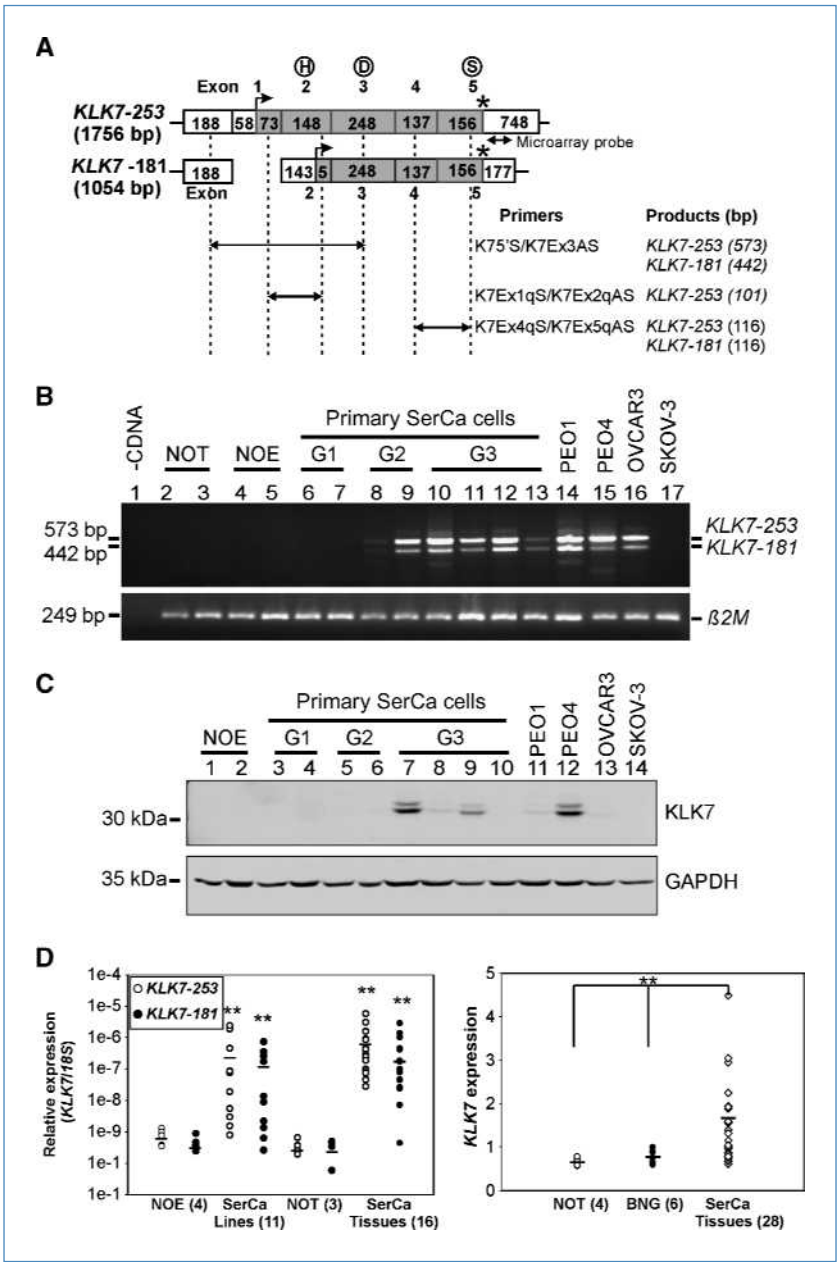

Figure 1. Expression of *KLK7* transcripts in serous EOC. A, schematic of *KLK7-253* (253 amino acids) and its variant, *KLK7-181* (181 amino acids). RT-PCR/RT-qPCR amplicons (arrowed lines), primers, size, and *KLK7* microarray oligo probes (arrowed line) are depicted. Arrow, ATG; asterisk, TAA. B, RT-PCR expression—*KLK7-253* and *KLK7-181* amplicons are 573 and 442 bp, respectively, with β2M as a loading control. Lane 1, no cDNA; lanes 2 and 3, NOT; lanes 4 and 5, NOE; lanes 6 and 7, primary serous EOC cells (grade 1); lanes 8 and 9, primary serous EOC cells (grade 2); lanes 10 to 13, primary serous EOC cells (grade 3); lanes 14 to 17, serous EOC cell lines. C, Western blots of KLK7 and GAPDH protein expression in EOC cells. Lanes 1 and 2, NOE; lanes 3 to 10, primary serous EOC cells (lanes 3 and 4, grade 1; lanes 5 and 6, grade 2; lanes 7–10, grade 3); lanes 11 to 14, serous EOC cell lines. D, left, RT-qPCR analysis of *KLK7-253* (exons 1–2; ○) and *KLK7-181* (●) expression; right, microarray analysis of relative *KLK7* mRNA levels in NOT, benign (BNG), and EOC tissues. *, $P < 0.001$.

~80% confluence. Spheroids were washed in PBS, incubated in CellTracker Green CMFDA (4 μmol/L; Invitrogen), added on top of mesothelial monolayers (approximately four to six spheroids/200 μL), and cultured at 37°C. At 4 h and 1, 2, and 3 d from the initial spheroid plating, images were taken as above. The experiment was performed thrice in quadruplicate.

Attachment assay. Attachment assays were performed using a published protocol (23) with 2×10^4 cells per well on plates coated (10 μg/mL) with fibronectin, vitronectin (BD Biosciences), and collagen I or IV (Calbiochem). For blocking assays, cells were seeded in serum-free medium with functional blocking β_1 integrin antibody or mouse IgG (10 μg/mL). The assay was repeated thrice with four replicates per ECM protein.

Flow cytometry

Cells (2×10^4) were incubated with primary integrin antibodies for 1.5 h with anti-mouse IgG as control, followed by Alexa-conjugated secondary antibodies, washed, and resuspended in 0.4 mL PBS before flow cytometry (Beckman Coulter) and data analysis using CXP software (Beckman Coulter). The experiment was repeated thrice per integrin.

Western blotting

Whole-cell lysates (20 μg) were separated by SDS-PAGE (15) and blotted with primary antibodies α_5 and β_1 (1:1,000)

integrins, KLK7 (1:500), and glyceraldehyde-3-phosphate dehydrogenase (GAPDH; 1:10,000) and secondary antibody IRDye 680/800–conjugated mouse/rabbit IgG (LI-COR Biosciences). Images were obtained using the Odyssey (LI-COR Biosciences) system, and densitometric analyses were performed using Odyssey software version 2.0.

Immunohistochemistry

Immunohistochemistry was performed as previously described (15) on paraffin-embedded sections of well-differentiated and poorly differentiated tumors from seven serous EOC patients who had responded or not to chemotherapy (ID nos. 7 and 11: nonresponders, poorly differentiated; ID nos. 28, 31, and 34: responders, poorly differentiated; ID nos. 23 and 37: responders, well differentiated; Supplementary Table S1). Following antigen retrieval and incubation with antibodies against KLK7 (1:200), α_5 or β_1 integrin (1:400), or rabbit IgG (negative control; Dako) overnight at 4°C, the EnVision peroxidase system (Dako) was applied. Sections were counterstained with Mayer's hematoxylin, visualized using a digital camera (Olympus BX41), and photographed (QCapture Pro 6.0 software). Images were processed using Adobe Photoshop CS3 and displayed using CorelDraw.

Results

KLK7-253 and *KLK7-181* are highly expressed in serous EOC cells and tissues

The relative expression levels and cancer specificity (15) of *KLK7-253* and *KLK7-181* transcripts were examined using a cohort of normal ovarian tissues (NOT), NOE, and serous EOC cells. In high-grade (G2 and G3) primary serous EOC cells, PEO1, PEO4, and OVCAR3 cell lines, two amplicons were observed, with *KLK7-253* bands (573 bp) generally more intense than those of *KLK7-181* (442 bp; Fig. 1B). In contrast, no amplicons were detected in NOT, NOE, low-grade (G1), or SKOV-3 cancer cells (Fig. 1B), with β2-microglobulin (β2M) as a loading control. KLK7 protein was also detected in lysates from three of four high-grade EOCs, PEO1 (faint bands), and PEO4 cell lines, but not NOE, low-grade cancer, or SKOV-3 cells (Fig. 1C). The two bands at approximately 32 to 35 kDa likely represent glycosylated and unglycosylated KLK7-253 (24). No bands were detected at the suspected ~20 kDa for the KLK7-181 isoform. RT-qPCR was performed for *KLK7-253* and *KLK7-181* transcripts using 4 NOE, 11 serous EOC lines, 3 NOT, and 16 serous EOC tissues. Both *KLK7* transcripts are significantly upregulated in EOC cells and tissues compared with NOE and NOT, respectively ($P < 0.001$; Fig. 1D, left). These data were supported by microarray analysis, which showed significantly higher total *KLK7* levels in cancerous than normal and benign ovarian tissues ($P < 0.001$; Fig. 1D, right).

KLK7-253 cells form MCAs that invade into mesothelial cell monolayers

MCA formation is thought to be a mechanism for EOC cell survival in ascites before peritoneal invasion (25, 26). To determine if KLK7 played a role in MCA formation, we generated stable transfectants of KLK7-253 and KLK7-181 in SKOV-3 cells (Supplementary Fig. S1B and C; Fig. 2A). Confocal microscopy confirmed protein over-expression in each of the KLK7-253 and KLK7-181 (at a lower level) clones, but negligible expression in vector control clones (Fig. 2A; Supplementary Fig. S1C). We then compared the ability of KLK7-253 and KLK7-181 clones to form spheroids (Fig. 2B). By 2, 4, and 7 days after seeding, vector controls and native SKOV-3 cells formed small spheroids compared with the single large compact MCA generated by all three KLK7-253 clones and less compact MCA formed by one (5D11) KLK7-181 clone (Fig. 2B). The other two KLK7-181 clones had a similar aggregation pattern to vector controls possibly due to low levels of KLK7-181 expression (Fig. 2A; Supplementary Fig. S1B and C).

We then examined the invasiveness of two representative MCAs (3E4 and 5D11) when added onto peritoneal mesothelial cell monolayers. As shown by bright-field and fluorescent imaging, both the compact KLK7-253 (3E4) and the less compact KLK7-181 (5D11) MCAs adhered on top of live mesothelial cell monolayers on the day of seeding and gradually formed an extensive front of invading cancer cells within 2 to 3 days (Fig. 2C), with the larger 3E4 MCA still spreading for up to 7 days (data not shown). However, similar migratory and invasive capacity of both KLK7-253 and KLK7-181 clones was apparent in two-dimensional Transwell migration and Matrigel invasion assays compared with vector controls (Supplementary Fig. S3A). Indeed, the attachment of KLK7-transfected clones to mesothelial cells did not differ from that of native SKOV-3 cells or vector controls (Supplementary Fig. S3B and C), suggesting that the only phenotypic difference induced by KLK7 overexpression was the ability to form MCAs.

KLK7-181 and KLK7-253 cell attachment to fibronectin/vitronectin is inhibited by a β1 integrin blocking antibody

To determine how disseminating KLK7-expressing cells invade into the peritoneum, given no difference in their adhesiveness to mesothelial cells (shown above), we examined their adhesion to ECM proteins from the matrix underlying mesothelial cell layers. Both KLK7-253 and KLK7-181 clones displayed increased adhesion to fibronectin and vitronectin (KLK7-181 only) compared with vector control cells (Fig. 3A and B), with greater adhesion exhibited by KLK7-181 clones ($P < 0.01$). There was no difference for collagen I/IV attachment (data not shown). The increased adhesion to fibronectin/vitronectin was reduced to basal levels by a β_1 integrin blocking antibody for KLK7-181 clones and less for KLK7-253 clones, especially on vitronectin [Fig. 3A and B; KLK7-181, $P < 0.01$; KLK7-253, $P < 0.05$ (fibronectin only)]. As both α_5 and β_1 integrins regulate MCA formation (7), we used these functional blocking antibodies in MCA assays. Blocking $\alpha_5\beta_1$, β_1, or KLK7 reduced aggregation of both KLK7-253 (3E4) and KLK7-181 (5D11) clones, whereas cells remained aggregated with an IgG control (Fig. 3C).

High α_5 integrin levels are associated with poor outcome for EOC patients (6), and increased α_5/β_1 integrins are responsible for serous EOC cell aggregation (7, 27), disaggregation, and invasion (8, 10). Of further interest, correlative analysis of our microarray data revealed a trend between *KLK7* and α_5 integrin

expression ($P = 0.09$). Thus, we investigated whether integrin levels were elevated in KLK7-expressing clones. Flow cytometric analysis showed significant upregulation of cell surface α_5 integrin expression in all KLK7-253 clones and β_1 and $\alpha_v\beta_3$ integrin expression in KLK7-253 4B12, 3F11, and KLK7-181 5D11 clones compared with vector control cells (Fig. 4A). Although there was not a strict correlation for all clones between α_5/β_1/KLK7 levels and MCA formation, KLK7-253 clones in particular expressed the highest KLK7, formed the most compact MCAs, and had increased α_5 (three of three) and β_1 (two of three) integrin levels.

KLK7 and α5/β1 integrins are coexpressed in serous primary EOC cells and tissues

To confirm the relationship between KLK7 and integrin expression clinically, we performed Western blot and densitometric analysis on paired samples of serous EOC cells from primary tumors and ascites from six women (Fig. 4B and C). Compared with primary EOC cells, three of six ascites samples (ID nos. 1, 3, and 5) showed more intense KLK7 bands, four of six ascites samples (ID nos. 1, 2, 3, and 5) showed more intense α_5 integrin bands (although this was not as apparent on densitometry), and two of six ascites samples (ID nos. 1 and 2) showed elevated β_1 integrin expression. Interestingly, levels of all three proteins (KLK7 and α_5 and β_1 integrins) were greater in ascites compared with primary tumor–derived cells from a patient who only survived 6 months (Fig. 4B and C; ID no. 1). Conversely, samples (ID nos. 4 and 6) from patients who survived 23 and 18 months, respectively, following surgery had little KLK7 and β_1 integrin but similarly intense α_5 integrin bands in their primary tumor–derived and ascites-derived cells.

Representative immunohistochemistry on serial sections of well-differentiated and poorly differentiated tumors from seven serous EOC patients who had responded or not to chemotherapy (Supplementary Table S1; Materials and Methods) is shown in Fig. 4D. Weak KLK7 and α_5/β_1 integrin immunostaining on the apical membrane was observed for both well-differentiated tumors that responded to chemotherapy (Fig. 4D, a, d, and g; ID no. 23). For poorly differentiated serous EOC tissues, two different immunostaining patterns were observed. Staining intensities for the responders were similar (KLK7), if not weaker (α_5/β_1), compared with well-differentiated tumors (Fig. 4D, b, e, and h; ID no. 34). Strikingly, however, the staining was more intense for all three antigens on tissues from the two patients who did not respond to chemotherapy (Fig. 4D, c, f, and i; ID no. 11). No staining was detected in the negative control (rabbit IgG; data not shown).

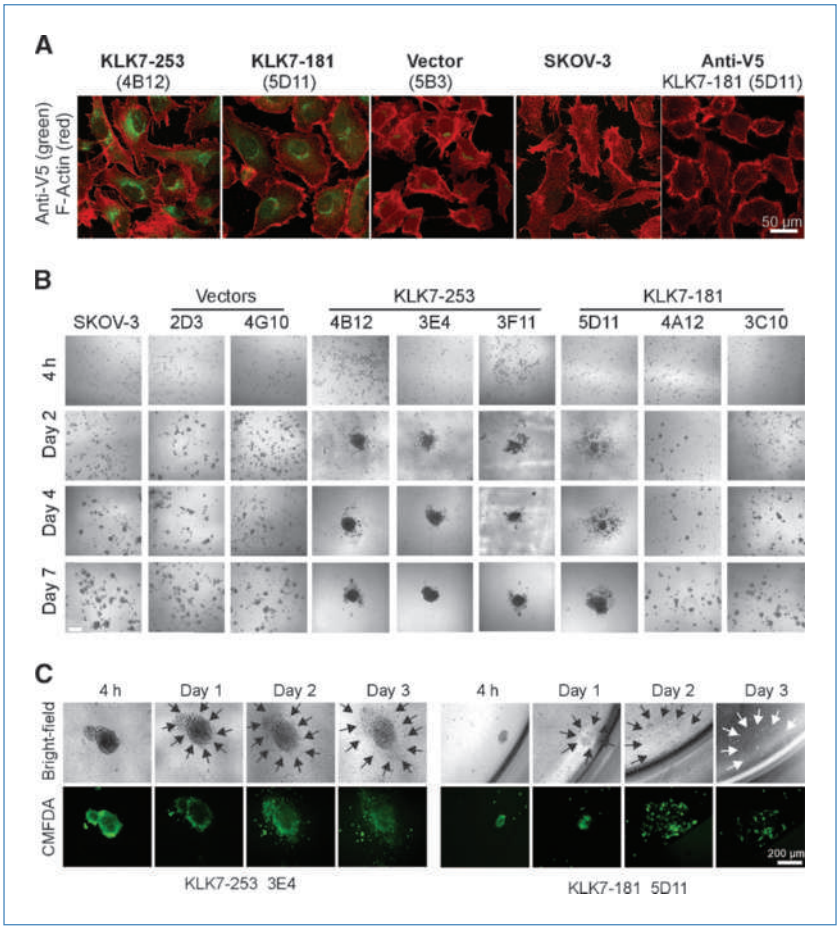

Figure 2. KLK7 overexpression promotes MCA/spheroids that invade into mesothelial monolayers. A, immunofluorescence using anti-V5 (green) antibody and phalloidin (red) confirmed V5-tagged KLK7 expression in SKOV-3 cells stably overexpressing KLK7-253 and KLK7-181 but not in vector control, native SKOV-3 cells, or negative control (primary antibody omitted). Scale bar, 50 μm. B, MCA/spheroid formation at 4 h and days 2, 4, and 7, with representative images of SKOV-3, vector control, KLK7-253, and KLK7-181 cells depicted. C, bright-field and immunofluorescence (CMFDA-labeled MCAs) images of 3E4 and 5D11 MCA invasion into mesothelial monolayers at 4 h and days 1, 2, and 3. Arrows, perimeters of invading MCAs.

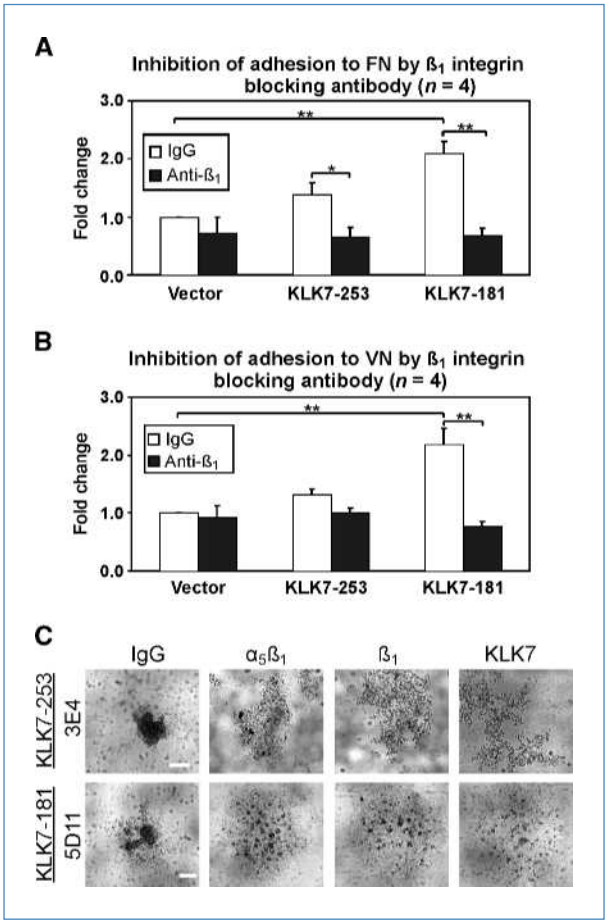

Figure 3. Adhesion to ECM and MCA formation was blocked by functional antibodies against α_5 and β_1 integrins and KLK7. Adhesion of KLK7-expressing cells to fibronectin (FN; A) and vitronectin (VN; B) and inhibition by a β_1 integrin blocking antibody. Data are from three clones of KLK7-253, KLK7-181, and vector controls. Columns, mean of four experiments; bars, SEM. *, $P < 0.05$; **, $P < 0.01$. C, representative images (day 2) from three experiments show inhibition of MCA formation by $\alpha_5\beta_1/\beta_1$ integrin and KLK7 blocking antibodies compared with mouse IgG control. Scale bar, 200 μm.

KLK7-expressing cells grow faster and are more resistant to paclitaxel

MCA formation of EOC cells is associated with increased resistance to certain chemotherapy regimens (9, 28, 29). Our clinical data (Supplementary Fig. S4; Supplementary Tables S1 and S3) and a previous report showed that patients who had shorter progression-free and overall survival time after surgery had increased *KLK7* expression (18). We then investigated if KLK7-expressing cells proliferate faster and how they respond to chemoreagents. Clones overexpressing NH_2-terminal truncated KLK7-181 grow faster than vector controls at 72 and 96 hours ($P < 0.05$), whereas KLK7-253 clones seemed to have increased proliferation without reaching significance (Fig. 5A). There was no significant difference in survival after cisplatin treatment (Fig. 5B), but both KLK7-253 and KLK7-181 cells showed less paclitaxel-induced cell death over the dose range of 1 to 100 nmol/L than vector controls ($P < 0.05$; Fig. 5C). Paclitaxel treatment of MCA/spheroids revealed that MCA-forming KLK7-253 (3E4) and KLK7-181 (5D11) clones are similarly more resistant toward paclitaxel ($P < 0.001$, 3E4; $P < 0.01$, 5D11) than the non–MCA-forming KLK7-181 (4A12) or vector cells (Fig. 5D). Although the non–MCA-forming 4A12 clone was more resistant to paclitaxel at 10 nmol/L ($P < 0.05$), resistance of both 3E4 and 5D11 MCAs is much higher. These data indicate that KLK7-induced chemoresistance to paclitaxel in two-dimensional monolayers is maintained in the MCAs formed in three-dimensional monolayers, suggesting one possible mechanism by which chemoresistance to paclitaxel is induced *in vivo*, leading to poorer patient outcome in KLK7-expressing EOCs.

Discussion

Approximately 75% of EOC patients are diagnosed with intra-abdominal dissemination (30). These patients are given platinum-paclitaxel chemotherapy after surgery, but most will develop resistance. Our work (Supplementary Fig. S4; Supplementary Table S3) confirmed that increased KLK7 expression is a hallmark (15) of EOC, particularly the serous subtype and an association between high KLK7 levels with high tumor grade, chemoresistance, and shorter survival time (16–18). We showed that KLK7 directs MCA formation and chemoresistance likely by upregulating $\alpha_5\beta_1$ integrin pathways. These observations indicate that KLK7 has potential not only as a prognostic marker for paclitaxel resistance but also as a therapeutic target in a subset of serous EOC patients who are paclitaxel nonresponders and have elevated KLK7 levels.

Expression of cell adhesion proteins, along with proteases, alters in EOC development (25, 26), although interaction between these molecules is more important during peritoneal invasion. The initiating step of EOC dissemination is that cells exfoliate from the primary site into the peritoneal cavity. KLK7 contributes to skin desquamation via degradation of cell adhesion glycoproteins (21), and thus, KLK7 may also help initiate EOC cell shedding by a similar mechanism. In pancreatic carcinoma, KLK7 cleaves E-cadherin to generate an ectodomain that promotes cell proliferation and invasion (31). Loss of E-cadherin and gain of α_5 integrin, a subunit of the major fibronectin receptor, have been related to an aggressive EOC phenotype (6). Interaction between $\alpha_4\beta_1$ integrin and vascular cell adhesion molecule-1 promotes EOC peritoneal metastasis (32); however, we did not see increased α_4 integrin in KLK7-expressing clones (data not shown). Collagen-binding integrins, such as $\alpha_2\beta_1$ and $\alpha_3\beta_1$, promote MMP9-dependent shedding of E-cadherin ectodomains (10). We did not see any evidence of E-cadherin processing in our KLK7-overexpressing clones nor changes in E-cadherin, N-cadherin, or cadherin 11/13 mRNA levels (data not shown). However, KLK7-253–expressing cells showed increased levels of cell surface α_5/β_1 integrins (Fig. 4A) from which we propose that $\alpha_5\beta_1$ integrins may promote the observed cell aggregation in these cells as previously reported (6, 7). Although integrins are classically thought to mediate cell-ECM adhesion, cell-cell adhesion can also be promoted (33). This is evidently the

mechanism seen here as no MCA was observed when α_5/β_1 integrins were inhibited (Fig. 5C). Compact MCAs are associated with an invasive EOC phenotype (34), and multicellular aggregation and disaggregation are regulated by MMP14 (35). Our data imply that other proteases, such as KLK7, are also involved by promoting EOC cell-cell adhesion in suspension via increased levels of α_5/β_1 integrins. Knocking down α_5/β_1 integrins reduced peritoneal seeding of ovarian cancer cells

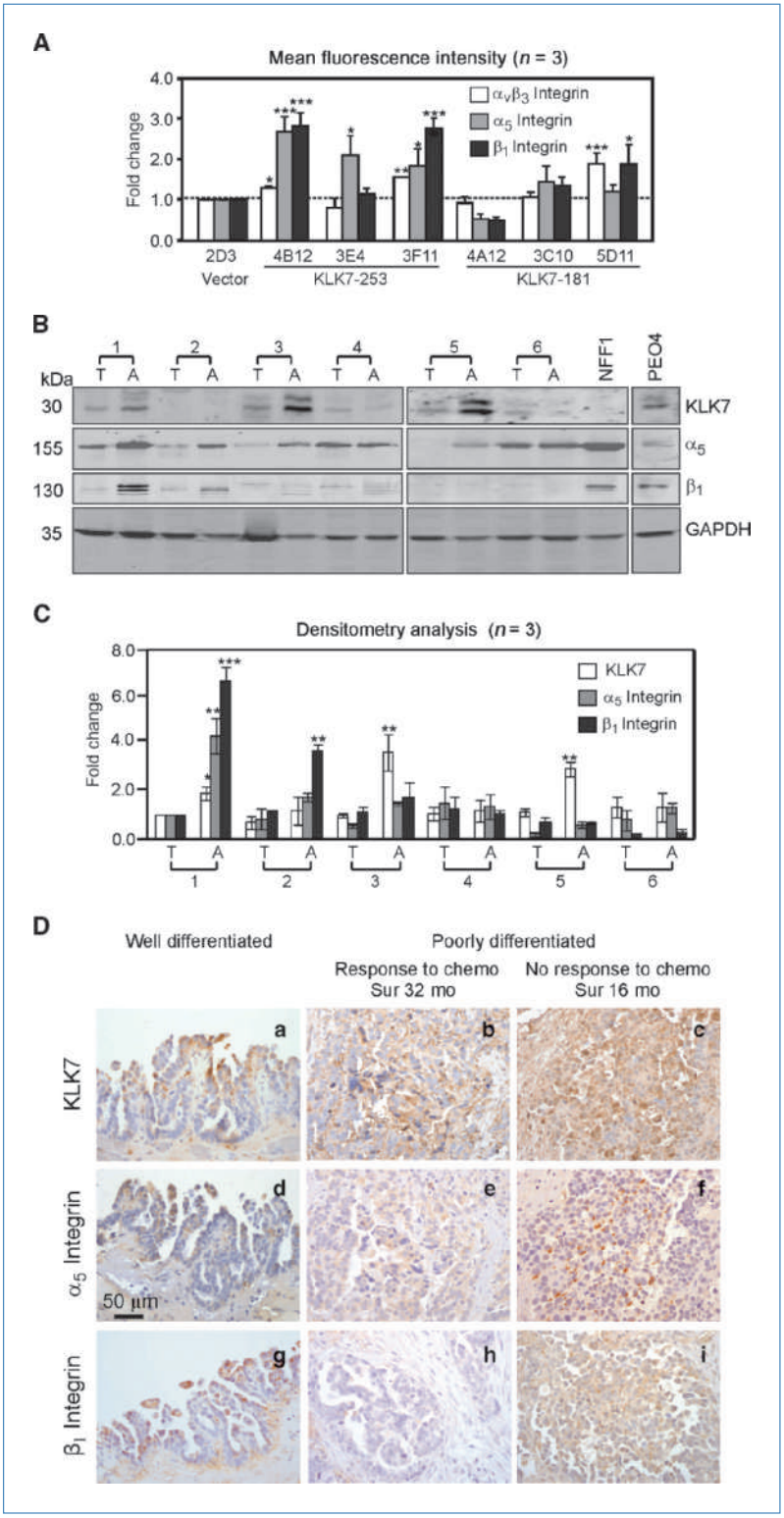

Figure 4. Enhanced expression of α_5/β_1 integrins in KLK7-expressing cells and clinical samples. A, flow cytometry analysis. Fold change of α_5/β_1 integrin expression of KLK7-253 and KLK7-181 clones compared with vector controls. Columns, mean fluorescence intensity ($n = 3$); bars, SEM. *, $P < 0.05$; **, $P < 0.01$; ***, $P < 0.001$. B, Western blots of KLK7 and α_5/β_1 integrin in six pairs of serous EOC cells from primary tumor (T) and ascites (A). GAPDH, loading control; PEO4 and NFF1, positive controls for KLK7 and integrins, respectively. C, densitometric analysis of three Western blots indicative of that shown in B. *, $P < 0.05$; **, $P < 0.01$; ***, $P < 0.001$. D, immunohistochemistry of KLK7 (a–c) and α_5 (d–f) and β_1 (g–i) integrin expression in tumor sections from two patients (ID nos. 23 and 34; Supplementary Table S1) with a well-differentiated (a, d, and g) or poorly differentiated (b, e, and h) tumor and who responded to chemotherapy and a poorly differentiated tumor (c, f, and i) from a chemotherapy nonresponder (ID no. 11). Scale bar, 50 μm.

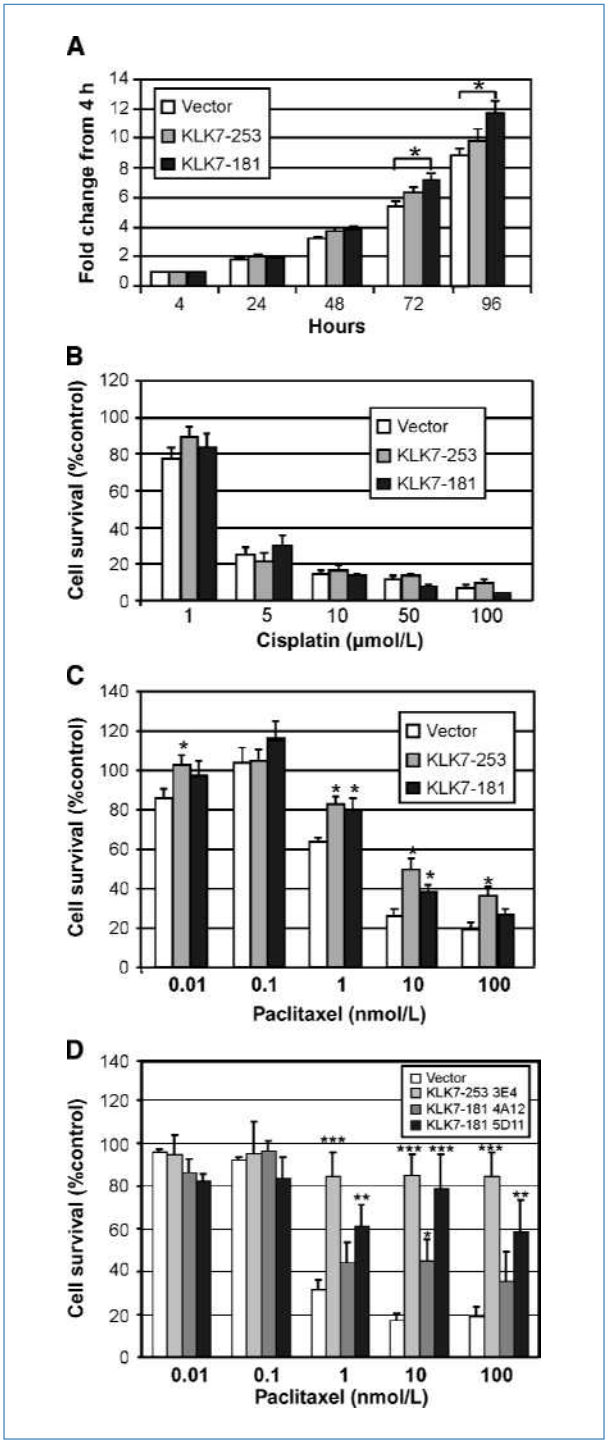

Figure 5. KLK7-253–expressing and KLK7-181–expressing cells are more resistant to paclitaxel. WST-1 assays were used to measure cell proliferation (A) and cell survival after cisplatin (1–100 μmol/L; B) and paclitaxel (0.01–100 nmol/L) treatment (C). Columns, mean of three clones each of KLK7-253, KLK7-181, and vector control cells; bars, SEM. D, paclitaxel treatment of MCAs from KLK7-253 (3E4), KLK7-181 (4A12 and 5D11), or vector control cells grown in three-dimensional suspension with cell survival measured using alamarBlue. Columns, mean of three assays performed in triplicate; bars, SEM. *, $P < 0.05$; **, $P < 0.01$; ***, $P < 0.001$.

(36), and thus, in conjunction with our data, KLK7 blocking might be an alternative therapeutic target for inhibiting serous EOC peritoneal invasion.

Inside the abdominal cavity, single cancer cells and MCAs/spheroids attach to the peritoneum composed of a single mesothelial cell layer over the ECM substrata. Collagen I/IV, vitronectin, and fibronectin are predominant components of the peritoneal ECM targeted by EOC cells (11, 37). KLK7-253 and, in particular, KLK7-181 clones displayed increased attachment to fibronectin/vitronectin (Fig. 3A and B). Interestingly, there is no increased adhesion of KLK7 cells to mesothelial cells grown in two-dimensional culture compared with vector cells (Supplementary Fig. S3B and C); nevertheless, MCAs formed by KLK7 cells attached to mesothelial cell layers and invaded to form cancer cell foci (Fig. 2C). Although mechanisms underlying interactions between MCAs and the peritoneal membrane remain unknown, in both *in vitro* omentum three-dimensional coculture and *in vivo* mouse models, EOC cells express and secrete more MMP2 that degrades peritoneal fibronectin and presumably increases tumor invasion (11), which may be one of the mechanisms observed here given the MMP2 activity seen on zymography (Supplementary Fig. S2B). Yet, KLK7 may be another protease that acts similarly; KLK7 degrades fibronectin to contribute to cell shedding (38) but reduces cell adhesion to vitronectin and enhances urokinase-type plasminogen activator receptor shedding in pancreatic carcinoma (39). This may be an additional mechanism in our study, as vitronectin adhesion was not increased to the same degree in KLK7-253 compared with KLK7-181 clones (Fig. 3B). Cytokines, including tumor necrosis factor and interleukin-1β, a KLK7 substrate (40), disrupt the peritoneal integrity by altering the morphology of mesothelial cells (41). This increases the exposure of the ECM (41) and promotes the invasion of attached malignant cells. Collectively, these findings may be reflected in more aggressive clinical phenotypes of patients with high KLK7-expressing and α_5/β_1 integrin–expressing tumors (Fig. 4B–D) observed here.

MCA/spheroid formation helps single cells overcome anoikis and to survive in an ascites suspension environment (25, 26). Paclitaxel resistance is also related to spheroid formation in three-dimensional suspension cultures (9, 29). Paclitaxel changes integrin expression, including $\alpha_5\beta_1$ integrin (42). Thus, the increased cell survival of KLK7-expressing cells with increased α_5/β_1 integrins following paclitaxel treatment may reflect the role of these ECM receptors in cellular responses to treatment (43) perhaps by the bcl-2 pathway, as both integrins suppress apoptosis via this mechanism (44). EOC cells exposed to paclitaxel accumulate at G_2-M and a sub-G_1 apoptotic phase when cultured as monolayers but not as spheroids. This relative sensitivity of two-dimensional monolayer cultures was associated with decreased bcl-X(L) levels after paclitaxel exposure but not in three-dimensional spheroids (9). MCAs are more resistant to chemotherapy than monolayers *in vitro* (9). However, in our hands, both KLK7-253 and KLK7-181 cells were less responsive to paclitaxel in either two-dimensional monolayers or three-dimensional MCAs (Fig. 5C and D), underscoring the robustness of KLK7-induced paclitaxel chemoresistance

and perhaps reflecting increased KLK7/α_5/β_1 levels seen in patients who were poor responders to chemotherapy (Fig. 4D; Supplementary Table S1).

Northern blot analyses showed two *KLK7* mRNA transcripts, *KLK7-253* and *KLK7-181*, in skin (45) and serous EOC cells (15). *KLK7-253* encodes the known active serine protease, whereas the exon 1–deleted *KLK7-181* variant (15) encodes an NH_2-terminal truncated KLK7-181 isoform that is not secreted or a protease. Its concurrently high expression with *KLK7-253* in EOC implies that this truncated KLK7-181 isoform has an adjunct intracellular function, although it is not yet detected at the protein level in clinical samples. We also could not determine the relative contribution (whether synergistic or dominant negative) of the KLK7-181 isoform from coculture experiments (Supplementary Fig. S2C), an attempt to mimic the simultaneous presence of both KLK7 variants in EOC. Nevertheless, although all KLK7-253 clones formed large MCAs, suggesting that proteolysis plays a role, one KLK7-181 clone (5D11) also formed spheroids (Fig. 4A), suggesting that proteolysis alone is not sufficient for MCA formation. That the functional KLK7 blocking antibody abolished MCA formation not only of KLK7-253 (4B12) clones but also of KLK7-181 (5D11) clones (Fig. 5C) further supports this notion. KLK7-181 cells showed increased proliferation (Fig. 5A) and increased adhesion to fibronectin/vitronectin (Fig. 3A and B), whereas KLK7-253 clones only showed increased attachment to fibronectin, further underscoring functional differences between both isoforms, which remain to be clarified. Native SKOV-3 cells treated with activated KLK7 enzyme also aggregated faster than those treated with the proteolytically inactive pro-KLK7 (Supplementary Fig. S2A), so presumably there are both proteolytic and nonproteolytic aspects of the functional roles of KLK7 isoforms. Notably, proteolytic-dependent and proteolytic-independent effects induced by prostasin, an extracellular serine protease, have been documented in prostate cancer cells (46); thus, there is precedence for this paradox.

In summary, we have confirmed that high KLK7 levels are indicative of poor outcome for EOC patients and, to our knowledge, for the first time have shown a link with paclitaxel chemoresistance. We have addressed a potential mechanism of action of KLK7 in EOC progression. Our data support the notion that the serine protease KLK7-253 and the NH_2-terminal truncated nonproteolytic KLK7-181 isoform promote MCAs, which are paclitaxel resistant. Increased levels of α_5/β_1 integrins in KLK7-expressing cells and intense staining of both integrins in EOC tissue sections with high KLK7 expression imply their association in promoting EOC cell dissemination and chemoresistance. Collectively, these findings suggest that KLK7 enhances the expression and function of integrin adhesion receptors and that both KLK7-253 and KLK7-181 isoforms function in EOC peritoneal invasion by mediating MCA and paclitaxel chemoresistance.

Disclosure of Potential Conflicts of Interest

No potential conflicts of interest were disclosed.

Acknowledgments

We thank Dr. Maria Brattsund (Umeå University, Umeå, Sweden) for the gift of KLK7 antibody and Dr. Michael McGuckin (Mater Medical Research Institute, Brisbane, Queensland, Australia) for access to the primary ovarian cells.

Grant Support

National Health and Medical Research Council (NHMRC) of Australia grants 242220, 390123, and 550523. J.A. Clements is a NHMRC Principal Research Fellow.

The costs of publication of this article were defrayed in part by the payment of page charges. This article must therefore be hereby marked *advertisement* in accordance with 18 U.S.C. Section 1734 solely to indicate this fact.

Received 09/16/2009; revised 01/17/2010; accepted 01/18/2010; published OnlineFirst 03/23/2010.

References

1. Jemal A, Siegel R, Ward E, et al. Cancer statistics, 2009. CA Cancer J Clin 2009;59:225–49.
2. Auersperg N, Wong AS, Choi KC, et al. Ovarian surface epithelium: biology, endocrinology, and pathology. Endocr Rev 2001;22:255–88.
3. Bast RC, Jr., Hennessy B, Mills GB. The biology of ovarian cancer: new opportunities for translation. Nat Rev Cancer 2009;9:415–28.
4. Hood JD, Cheresh DA. Role of integrins in cell invasion and migration. Nat Rev Cancer 2002;2:91–100.
5. Goldberg I, Davidson B, Reich R, et al. α_v Integrin expression is a novel marker of poor prognosis in advanced-stage ovarian carcinoma. Clin Cancer Res 2001;7:4073–9.
6. Sawada K, Mitra AK, Radjabi AR, et al. Loss of E-cadherin promotes ovarian cancer metastasis via α_5-integrin, which is a therapeutic target. Cancer Res 2008;68:2329–39.
7. Casey RC, Burleson KM, Skubitz KM, et al. β_1-Integrins regulate the formation and adhesion of ovarian carcinoma multicellular spheroids. Am J Pathol 2001;159:2071–80.
8. Burleson KM, Hansen LK, Skubitz AP. Ovarian carcinoma spheroids disaggregate on type I collagen and invade live human mesothelial cell monolayers. Clin Exp Metastasis 2004;21:685–97.
9. Frankel A, Buckman R, Kerbel RS. Abrogation of taxol-induced G_2-M arrest and apoptosis in human ovarian cancer cells grown as multicellular tumor spheroids. Cancer Res 1997;57:2388–93.
10. Symowicz J, Adley BP, Gleason KJ, et al. Engagement of collagen-binding integrins promotes matrix metalloproteinase-9-dependent E-cadherin ectodomain shedding in ovarian carcinoma cells. Cancer Res 2007;67:2030–9.
11. Kenny HA, Kaur S, Coussens LM, et al. The initial steps of ovarian cancer cell metastasis are mediated by MMP-2 cleavage of vitronectin and fibronectin. J Clin Invest 2008;118:1367–79.
12. Clements JA, Willemsen NM, Myers M, et al. The tissue kallikrein family of serine proteases: functional roles in human disease and potential as clinical biomarkers. Crit Rev Clin Lab Sci 2004;41:265–312.
13. Borgono CA, Diamandis EP. The emerging roles of human tissue kallikreins in cancer. Nat Rev Cancer 2004;4:876–90.
14. Pampalakis G, Sotiropoulou G. Tissue kallikrein proteolytic cascade pathways in normal physiology and cancer. Biochim Biophys Acta 2007;1776:22–31.
15. Dong Y, Kaushal A, Brattsand M, et al. Differential splicing of KLK5 and KLK7 in epithelial ovarian cancer produces novel variants with potential as cancer biomarkers. Clin Cancer Res 2003;9:1710–20.
16. Kyriakopoulou LG, Yousef GM, Scorilas A, et al. Prognostic value of

quantitatively assessed KLK7 expression in ovarian cancer. Clin Biochem 2003;36:135–43.
17. Psyrri A, Kountourakis P, Scorilas A, et al. Human tissue kallikrein 7, a novel biomarker for advanced ovarian carcinoma using a novel *in situ* quantitative method of protein expression. Ann Oncol 2008; 19:1271–7.
18. Shan SJ, Scorilas A, Katsaros D, et al. Unfavorable prognostic value of human kallikrein 7 quantified by ELISA in ovarian cancer cytosols. Clin Chem 2006;52:1879–86.
19. Hibbs K, Skubitz KM, Pambuccian SE, et al. Differential gene expression in ovarian carcinoma: identification of potential biomarkers. Am J Pathol 2004;165:397–414.
20. Tanimoto H, Underwood LJ, Shigemasa K, et al. The stratum corneum chymotryptic enzyme that mediates shedding and desquamation of skin cells is highly overexpressed in ovarian tumor cells. Cancer 1999; 86:2074–82.
21. Caubet C, Jonca N, Brattsand M, et al. Degradation of corneodesmosome proteins by two serine proteases of the kallikrein family, SCTE/KLK5/hK5 and SCCE/KLK7/hK7. J Invest Dermatol 2004; 122:1235–44.
22. Newton TR, Parsons PG, Lincoln DJ, et al. Expression profiling correlates with treatment response in women with advanced serous epithelial ovarian cancer. Int J Cancer 2006;119:875–83.
23. Romanov VI, Goligorsky MS. RGD-recognizing integrins mediate interactions of human prostate carcinoma cells with endothelial cells *in vitro*. Prostate 1999;39:108–18.
24. Ekholm IE, Brattsand M, Egelrud T. Stratum corneum tryptic enzyme in normal epidermis: a missing link in the desquamation process? J Invest Dermatol 2000;114:56–63.
25. Shield K, Ackland ML, Ahmed N, et al. Multicellular spheroids in ovarian cancer metastases: biology and pathology. Gynecol Oncol 2009;113:143–8.
26. Tan DS, Agarwal R, Kaye SB. Mechanisms of transcoelomic metastasis in ovarian cancer. Lancet Oncol 2006;7:925–34.
27. Shield K, Riley C, Quinn MA, et al. $\alpha_2\beta_1$ Integrin affects metastatic potential of ovarian carcinoma spheroids by supporting disaggregation and proteolysis. J Carcinog 2007;6:11.
28. Minchinton AI, Tannock IF. Drug penetration in solid tumours. Nat Rev Cancer 2006;6:583–92.
29. Makhija S, Taylor DD, Gibb RK, et al. Taxol-induced bcl-2 phosphorylation in ovarian cancer cell monolayer and spheroids. Int J Oncol 1999;14:515–21.
30. Fishman DA, Borzorgi K. Cancer treatment and research. In: Stack MS, Fishman DA, editors. Ovarian cancer. Boston: Kluwer Academic Publishers; 2002, p. 3–28.
31. Johnson SK, Ramani VC, Hennings L, et al. Kallikrein 7 enhances pancreatic cancer cell invasion by shedding E-cadherin. Cancer 2007;109:1811–20.
32. Slack-Davis JK, Atkins KA, Harrer C, et al. Vascular cell adhesion molecule-1 is a regulator of ovarian cancer peritoneal metastasis. Cancer Res 2009;69:1469–76.
33. Whittard JD, Akiyama SK. Activation of β_1 integrins induces cell-cell adhesion. Exp Cell Res 2001;263:65–76.
34. Sodek KL, Ringuette MJ, Brown TJ. Compact spheroid formation by ovarian cancer cells is associated with contractile behavior and an invasive phenotype. Int J Cancer 2009;124:2060–70.
35. Moss NM, Barbolina MV, Liu Y, et al. Ovarian cancer cell detachment and multicellular aggregate formation are regulated by membrane type 1 matrix metalloproteinase: a potential role in i.p. metastatic dissemination. Cancer Res 2009;69:7121–9.
36. Yokoyama Y, Sedgewick G, Ramakrishnan S. Endostatin binding to ovarian cancer cells inhibits peritoneal attachment and dissemination. Cancer Res 2007;67:10813–22.
37. Witz CA, Montoya-Rodriguez IA, Cho S, et al. Composition of the extracellular matrix of the peritoneum. J Soc Gynecol Investig 2001;8:299–304.
38. Ramani VC, Haun RS. The extracellular matrix protein fibronectin is a substrate for kallikrein 7. Biochem Biophys Res Commun 2008;369: 1169–73.
39. Ramani VC, Haun RS. Expression of kallikrein 7 diminishes pancreatic cancer cell adhesion to vitronectin and enhances urokinase-type plasminogen activator receptor shedding. Pancreas 2008;37:399–404.
40. Nylander-Lundqvist E, Egelrud T. Formation of active IL-1β from pro-IL-1β catalyzed by stratum corneum chymotryptic enzyme *in vitro*. Acta Derm Venereol 1997;77:203–6.
41. Stadlmann S, Pollheimer J, Renner K, et al. Response of human peritoneal mesothelial cells to inflammatory injury is regulated by interleukin-1β and tumor necrosis factor-α. Wound Repair Regen 2006;14:187–94.
42. Bhan V, Mader JS, Hoskin DW. *In vitro* exposure to paclitaxel modulates integrin expression by human T lymphocytes and inhibits T cell adhesion to breast carcinoma cells. Oncol Rep 2004;11: 893–7.
43. Zutter MM. Integrin-mediated adhesion: tipping the balance between chemosensitivity and chemoresistance. Adv Exp Med Biol 2007;608: 87–100.
44. Zhang Z, Vuori K, Reed JC, et al. The α5β1 integrin supports survival of cells on fibronectin and up-regulates Bcl-2 expression. Proc Natl Acad Sci U S A 1995;92:6161–5.
45. Hansson L, Stromqvist M, Backman A, et al. Cloning, expression, and characterization of stratum corneum chymotryptic enzyme. A skin-specific human serine proteinase. J Biol Chem 1994;269: 19420–6.
46. Chen M, Fu YY, Lin CY, et al. Prostasin induces protease-dependent and independent molecular changes in the human prostate carcinoma cell line PC-3. Biochim Biophys Acta 2007;1773:1133–40.